Understanding the structural disorganization of starch in water–ionic liquid solutions

Binjia Zhang,[a,b] Ling Chen,[b] Fengwei Xie,[*a] Xiaoxi Li,[b] Rowan W. Truss,[c] Peter J. Halley,[a,c] Julia L. Shamshina,[d] Robin D. Rogers,[d] Tony McNally[e]

[a] *Australian Institute for Bioengineering and Nanotechnology, The University of Queensland, Brisbane, Qld 4072, Australia*

[b] *Ministry of Education Engineering Research Center of Starch & Protein Processing, Guangdong Province Key Laboratory for Green Processing of Natural Products and Product Safety, College of Light Industry and Food Sciences, South China University of Technology, Guangzhou 510640, China*

[c] *School of Chemical Engineering, The University of Queensland, Brisbane, Qld 4072, Australia*

[d] *Center for Green Manufacturing and Department of Chemistry, The University of Alabama, Tuscaloosa, AL 35487-0336, USA*

[e] *International Institute for Nanocomposites Manufacturing (IINM), WMG, University of Warwick, CV4 7AL, UK*

[*] Corresponding author. Tel.: +61 7 3346 3199; fax: +61 7 3346 3973.

Email address: f.xie@uq.edu.au; fwhsieh@gmail.com (F. Xie)

Abstract

Using synchrotron X-ray scattering analyses and Fourier transform infrared spectroscopy, this work provides insights into the solvent effects of water:[C_2mim][OAc] solutions on the disorganization of starch semi-crystalline structure. When a certain ratio (10.2:1 mol/mol) of water:[C_2mim][OAc] solution is used, the preferential hydrogen bonding between starch hydroxyls and $[OAc]^-$ anion results in the breakage of the hydrogen bonding network of starch and thus the disruption of starch lamellae. This greatly facilitates the disorganization of starch, which happens much easier than in pure water. In contrast, when 90.8:1 (mol/mol) water:[C_2mim][OAc] solution is used, the interactions between $[OAc]^-$ anion and water suppress the solvent effects on starch, making less easy the disorganization of starch than in pure water. All these differences can be shown by changes in the lamellar and fractal structures: firstly, a preferable increase in the thickness of the crystalline lamellae rather than that of the amorphous lamellae causes an overall increase in the thickness of the semi-crystalline lamellae; then, the amorphous lamellae starts to decrease probably due to the out-phasing of starch molecules from them; this forms fractal gel on a larger scale (than the lamellae) which gradually decreases to a stable value as the temperature increases further. It is noteworthy that these changes happen at temperatures far below the transition temperature that is thermally detectable as is normally described. This hints to our future work that using certain aqueous ionic liquids for destructuration of starch semi-crystalline structure is the key to realize green processes to obtain homogeneous amorphous materials.

1. Introduction

With the utilization of renewable resources becoming the focus of industry, there has been huge interest in the design and application of innovative technology for converting these renewable feed-stocks into desirable forms.[1, 2] Polymers from renewable resources have attracted great attention due to their availability, renewability, biocompatibility, and biodegradability.[3] Among these renewable polymers which are potential alternatives to traditional petroleum-based polymers, starch, as a biopolymer from agro-sources, has attracted intense interest especially for developing biodegradable plastics.[4] Regarding this, great efforts have been made to improve the processes to obtain starch-based products with desirable structure and better performance.[5-7]

For utilization of starch, it is significant to understand the unique structure of starch. Naturally in plants, it exists in the form of granules (<1 μm~100 μm in size); each granule is composed of alternating amorphous and semi-crystalline shells (growth rings) (100~400 nm in size); and the semi-crystalline shell is stacked by crystalline and amorphous lamellae (periodicity, 9~10 nm). Starch consists of two major biomacromolecules called amylose (mainly linear) and amylopectin (hyper-branched) (~nm).[8-11] Native starch has low solubility in conventional solvents despite its highly hydrophilic nature due to strong hydrogen bonding between the strands of starch; although its 3D semi-crystalline structure may be slightly disrupted in excess of water at elevated temperatures, a process known as "gelatinization". However, while some starch molecules (mainly amylose) can be dissolved in water during gelatinization, there are always granule remnants present in the gelatinized products.[12] Therefore, when trying to obtain homogenous amorphous materials from starch, its insolubility presents an issue.

Ionic liquids (ILs), now commonly defined as salts having low melting points (<100 °C),[13] have recently attracted much interest for aiding the processing of polysaccharides like starch. Many ILs, especially ones based on the basic anions, have been shown to be capable of dissolving biopolymers,

including starch.[14] When the effect of IL anions was investigated, the acetate anion, $[OAc]^-$ was identified as the most effective,[15-17] which follows Hofmeister series for anions.[18] Therefore, imidazolium acetate ILs can dissolve polysaccharides such as starch and thus can be used as excellent media for polysaccharide solubilization and modification.[19-22] Moreover, the use of ILs could also allow the development of starch-based ionically conducting polymers or solid polymer electrolytes.[23-29]

It is worth noting that many of the ILs used previously to dissolve starch contained anions with efficient basicity, but which were corrosive like $[Cl]^-$ anion (*e.g.,* $[C_4mim][Cl]$).[22] Besides the corrosiveness issue, macromolecular degradation of starch can be observed,[30, 31] due to the acidic hydrolysis of starch glycosidic bonds. Specifically, the reason for this degradation is the formation of HCl (as a result of the protonation of $[Cl]^-$ anion in the presence of moisture), which can catalyze the depolymerization of starch.[31] Considering this issue, more recent studies have been focused on ILs with non-halogenated anions, such as 1-ethyl-3-methylimidazolium acetate ($[C_2mim][OAc]$).[32-34] The IL $[C_2mim][OAc]$ has very low vapor pressure, high thermal stability, and relatively low viscosity at room temperature,[33] and has been found to be much less aggressive for degrading starch.[34] Moreover, it has been found that the transition (gelatinization and/or dissolution) temperature and enthalpy of starch can be modulated by using $[C_2mim][OAc]$ mixed with different amounts of water.[32, 34] In particular, when a certain ratio of water:$[C_2mim][OAc]$ is used, starch can be transformed into a homogeneous gel at much reduced temperature close to room temperature (RT).[32, 34] While this provides a promising method for starch processing with much reduced energy input, the detailed mechanism that regulates starch transitions by water:$[C_2mim][OAc]$ solutions has yet to be understood. Sciarini *et al.* suggested that the mild starch depolymerization by $[C_2mim][OAc]$ may facilitate starch swelling, accounting for the shifting of the gelatinization transition towards lower temperatures. However, as starch has a complex supra-molecular semi-crystalline structure, to fully understand the solvent effects of water:$[C_2mim][OAc]$ solutions on the starch transition,

examining how the solutions alter the way the starch semi-crystalline structure changes during the transition is necessary.

As "green solvents", ILs or IL-water solutions have been confirmed to be efficient at destructurizing lignocellulosic biomass[35] (e.g., pine,[36, 37] willow,[38] and switchgrass[39]) for the production of renewable fuels, chemicals and materials, which can be well probed using analytical tools spanning multiple length scales including spectroscopies,[40] and small-angle X-ray scattering (SAXS) and wide-angle X-ray scattering (WAXS) techniques.[41] We have shown earlier that when the IL ([C_2mim][OAc]) dissolves the switchgrass, not all of the physical and chemical (covalent entanglements linkages) interactions between the biomass components get disrupted during the process.[42] In order to look whether this is the case in starch, investigate the solvent effects of water:[C_2mim][OAc] solutions on this polymer and rationalize these effects, the current work used temperature-resolved SAXS and WAXS techniques to monitor starch structural changes in water:[C_2mim][OAc] solutions, combined with Fourier-transform infrared spectroscopy (FT-IR) to understand the related molecular interactions.

2. Experimental

2.1. Materials

Waxy maize starch, with an amylose content of 3.4 wt% (measured by Tan *et al.*[43] using the iodine colorimetric method) and an initial moisture content of 12.4 wt%, was purchased from New Zealand Starch Ltd. (Onehunga, Auckland, New Zealand). Milli-Q water was used in all instances. The [C_2mim][OAc] IL, of ≥ 95% purity (with water content *ca.* 1200 ppm), produced by IoLiTec Ionic Liquids Technologies GmbH (Salzstraβe184, D-74076 Heilbronn, Germany), was supplied by Chem-Supply Pty Ltd (Gillman, SA, Australia). As [C_2mim][OAc] is a liquid and is miscible with water at room temperature,[44] water:[C_2mim][OAc] solutions of different ratios (9:1, 7:3 and 1:1 wt/wt) could be easily prepared in vials for subsequent studies (Table S1). These weight ratios

correspond to mole ratios of 90.8:1, 23.6:1, 10.2:1 mol/mol, also presented in Table S1. The purity and water content of the chemicals were considered for mole ratio calculations. Anhydrous sodium acetate (NaOAc), ≥ 99% purity, was supplied by Sigma-Aldrich Pty Ltd (Castle Hill, NSW 1765, Australia).

Please note that the solutions with more than 50 wt% [C_2mim][OAc] have not been used in this work due to the their ability to rapidly change the starch structure without any thermal treatment, which made the synchrotron work difficult. However, this phenomenon will be investigated in follow-up studies.

2.2. Differential scanning calorimetry (DSC)

A TA Q2000 DSC (TA Instruments, Inc., New Castle, DE, USA) was used to investigate the thermal transition of native starches in water:[C_2mim][OAc] solutions. The instrument was calibrated using indium as a standard (melting point of 155.6 °C). Starch in the amount of 1.5–3 mg was weighed into the 40 μL Tzero aluminium pan (TA Instruments, Inc. New Castle, DE, USA), to which was then added, by a micro-syringe, the water:[C_2mim][OAc] solution, in the amount 10 times that of the starch. Then, a pin was used to gently mix starch with the solution. After sealing, the pan was gently shaken for a few seconds. The mixing and shaking were to ensure the starch granules were completely immersed and equally dispersed in the liquid but did not sediment at the bottom of the pan. The pans thus prepared were transferred into the DSC machine for immediate analysis to avoid sedimentation of starch granules or time effects of the water:[C_2mim][OAc] solution on starch. An empty pan was used as a reference. The pans were heated from 20 °C to 120 °C at a scanning rate of 5 °C/min. At least two runs were carried out for each sample to ensure the consistency of the results. The Universal Analysis 2000 (TA Instruments–Waters LLC) software was used to analyze the main gelatinization endotherm of the DSC traces for the onset (T_o), peak (T_p), and conclusion (T_c) temperatures.

2.3. Synchrotron small/wide angle X-ray scattering (SAXS/WAXS) analyses

Temperature-resolved SAXS and WAXS analyses were carried out on the SAXS/WAXS beamline (flux, 10^{13} photons/s) at the Australian Synchrotron (Clayton, Vic, Australia), at a wavelength λ = 1.47 Å. The 2D scattering patterns were collected using a Pilatus 1M camera (active area 169 × 179 mm; and pixel size 172× 172 μm) and a Pilatus 200K camera (active area 169 × 33 mm; and pixel size 172 × 172 μm). The scatterBrain software was used to acquire the one-dimensional (1D) data from the 2D scattering pattern, and the data in the angular ranges of $0.015 < q < 0.15$ Å^{-1} and $0.095 < q < 2$ Å^{-1} were used as the SAXS and WAXS patterns, respectively, in which $q = 4\pi\sin\theta/\lambda$ (where 2θ is the scattering angle and λ is the wavelength of the X-ray source). All the data were background subtracted and normalized.

Starch suspensions with a starch concentration of 10 wt% were prepared by adding a desired amount of the water:[C_2mim][OAc] solution to the starch (the mole ratios of components are shown in Table S1). The starch suspensions were injected into quartz capillaries of 1 mm diameter (Hilgenberg Gmbh, Germany), which were then placed on a multi-capillary hot-stage provided by the Australian Synchrotron. After equilibration at 28 °C, the starch suspensions were heated from 28 °C to 66 °C (slightly higher than the onset gelatinization temperature (T_o) of the starch in pure water) at a rate of *ca.* 1 °C/min, and the SAXS/WAXS data were recorded every 2 °C for an acquisition time of 1 s. Furthermore, the SAXS/WAXS patterns were also recorded for all the three samples at 74 °C and 76 °C, when the starch in 10.2:1 mol/mol solution was fully destructured.

SAXS data recorded from 28 to 66 °C were fitted using a power-law (Gaussian) function, as shown in Eq. (1) below.

$$I(q) = B + Pq^{-\alpha} + \frac{A\sqrt{\ln 4}}{W\sqrt{\pi/2}} \exp\left(-\frac{2\ln 4\left(q - q_0\right)^2}{W^2}\right) \quad (1)$$

where the first term B is the background; the second term is the power-law function where P is the power-law pre-factor and α is the power-law exponent; the third term is a Gaussian function where A is the peak area, W (Å^{-1}) the full width at half maximum (FWHM, a reciprocal space parameter indicating the polydispersity of the semi-crystalline lamellae) in reciprocal space, and q_0 (Å^{-1}) the peak center position.[45, 46]

Data fitting was performed using least-square refinement in the NCNR analysis macros.[46] The fitting curve for the starch in pure water at 28 °C, by way of an example, is shown in Fig. S1. The FWHM in reciprocal space was converted to that in real space using Eq. (2):

$$\text{FWHM(real)} = \frac{2\pi W}{{q_0}^2} \tag{2}$$

The linear correction function $L(r)$, as given in Eq. (3) (below) and Fig. S2, was used to study the parameters of the starch lamellar structure.

$$L(r) = \frac{\int_0^\infty I(q)q^2\cos(qr)\mathrm{d}q}{\int_0^\infty I(q)q^2\mathrm{d}q} \tag{3}$$

In Eq. (3), r (nm) is the distance in real space; and in Fig. S2, d is the second maximum of $L(r)$ (the repeating distance, *i.e.*, the thickness of semi-crystalline lamellae). Fig. S2 also shows a parameter d_a, representing the average thickness of amorphous lamellae within the semicrystalline lamellae, which can be acquired by the solution of the linear region and the flat $L(r)$ minimum. Thus, d_c, the average thickness of crystalline lamellae can be calculated by $d_c = d - d_a$.

For the SAXS patterns recorded at 62 °C, 64 °C, 66 °C, 74 °C and 76 °C for the partially melted starch in pure water and 90.8:1 mol/mol solutions, and the fully melted starch in the 10.2:1 mol/mol solution, the data in the range of $0.045 < q < 0.15$ Å^{-1} were also fitted using Eq. (1) to obtain the

power-law exponent α (re-represented as α_1), and the data in the range of q < 0.045 Å^{-1} were fitted using an unified model (Eq. (4)) to the power-law exponent δ:

$$I(q) = G\exp\left(-\frac{R_g^2 q^2}{3}\right) + C\left(\frac{(\mathrm{efr}(qR_g/\sqrt{6}))^3}{q}\right)^{\delta} \quad (4)$$

Here, G is the pre-factor of the Guinier function corresponding to a radius R_g, and C and δ are the pre-factor and the exponent of the power-law function, respectively.

2.4. Attenuated total reflectance Fourier-transform infrared (ATR-FTIR) spectroscopy

Infrared spectra were collected for the water:[C_2mim][OAc] solutions without starch and for these solutions with 10 wt% starch heated at 76 °C for 30 min. The ATR-FTIR spectra were recorded using a Nicolet 5700 FTIR spectrometer (Thermo Electron Corp, Madison, WI, USA) equipped with a Nicolet Smart Orbit ATR accessory incorporating a diamond internal reflection element. Spectra were collected at a resolution of 4 cm^{-1} in the range of 4000–400 cm^{-1} for a total of 64 scans for all the samples. ATR-FTIR spectra were baseline corrected and normalized before further analysis.

3. Results and Discussion

3.1. Differential scanning calorimetry (DSC)

For understanding the thermally induced transitions of a polymer, differential scanning calorimetry (DSC) is the most suitable technique. Thus, the DSC thermograms for waxy maize starch (10 wt% concentration) suspended in pure water and 90.8:1 and 10.2:1 mol/mol solutions were studied (see Fig. 1). While heated in pure water, the starch displayed a prominent endothermic transition indicating gelatinization (T_o: 65 °C; T_p: 72 °C; T_c: 84 °C). When the 90.8:1 mol/mol solution was used instead as the solvent, the transition peak shifted upwards (T_o: 74 °C; T_p: 80 °C; T_c: 91 °C); in contrast, when much less water was used, *e.g.*, in the 10.2:1 mol/mol solution, the endothermic

transition of starch occurred at a much lower temperature (T_o: 57 °C; T_p: 63 °C; T_c: 72 °C), even lower than in pure water. These results clearly indicate that water:[C_2mim][OAc] solutions were capable of regulating the transition temperature of starch. Based on these results, the solvent effects of water:[C_2mim][OAc] solutions on starch polymers were then explored from a semi-crystalline structural perspective, which would promote the rational application of water/IL solutions in using starch polymers with controllable transition behavior and resulting material structure and properties.

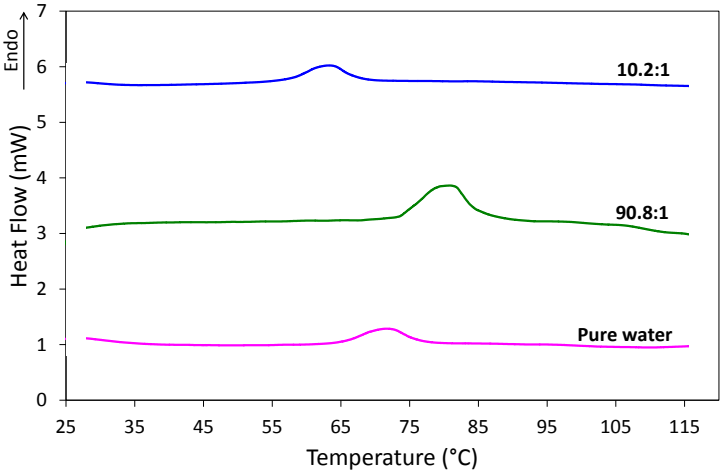

Fig. 1 DSC thermograms for the starch in pure water (pink) and 90.8:1 (green) and 10.2:1 mol/mol (blue) water:[C_2mim][OAc] solutions.

3.2. Temperature-resolved wide-angle X-ray scattering (WAXS) analysis

Different types of starch show different WAXS patterns determined by their crystalline regions.[47] Fig. 2 shows the influence of water:[C_2mim][OAc] solutions on the crystalline structure during thermal treatment using temperature-resolved WAXS. The starch exhibited the A-type polymorph, characterized by main peaks at 10.64 $Å^{-1}$, 12.03 $Å^{-1}$, 12.75 $Å^{-1}$ and 16.25 $Å^{-1}$ (Cu K_α 2θ: 15°, 17°, 18° and 23°).[48, 49] With the temperature increased to 66 °C, an apparent gradual reduction in WAXS peak intensities could be observed for the starch in pure water. The 10.2:1 mol/mol solution resulted in more prominently reduced peaks, whereas the least significant weakening of the peaks was seen

for the 90.8:1 mol/mol solution. As the sharp WAXS peaks are related to starch crystallites and the dispersive patterns correspond to the amorphous starch,[50] the results were in agreement with the previous DSC results and affirmed the ability of water:[C_2mim][OAc] solutions to adjust the melting temperature of starch crystallites. Specifically, when the temperature was over 64 °C, all the crystallites were melted by the 10.2:1 mol/mol solution (no peaks presented). When pure water and the 90.8:1 mol/mol solution were used, residual crystallites could still be detected, with slightly more crystallites remaining for the starch in the 90.8:1 mol/mol solution than in pure water. Starch crystallites at the long-range scale mainly consist of monoclinic and/or hexagonal crystal units, containing short-range double-helices and inter-helical water molecules which are organized together through a large amount of inter- and intra-molecular hydrogen bonding.[51] Thus, it is proposed that the changes of starch crystallites during thermal treatment resulted from the breakage of the hydrogen bonding network at a molecular level by the water:[C_2mim][OAc] solutions.

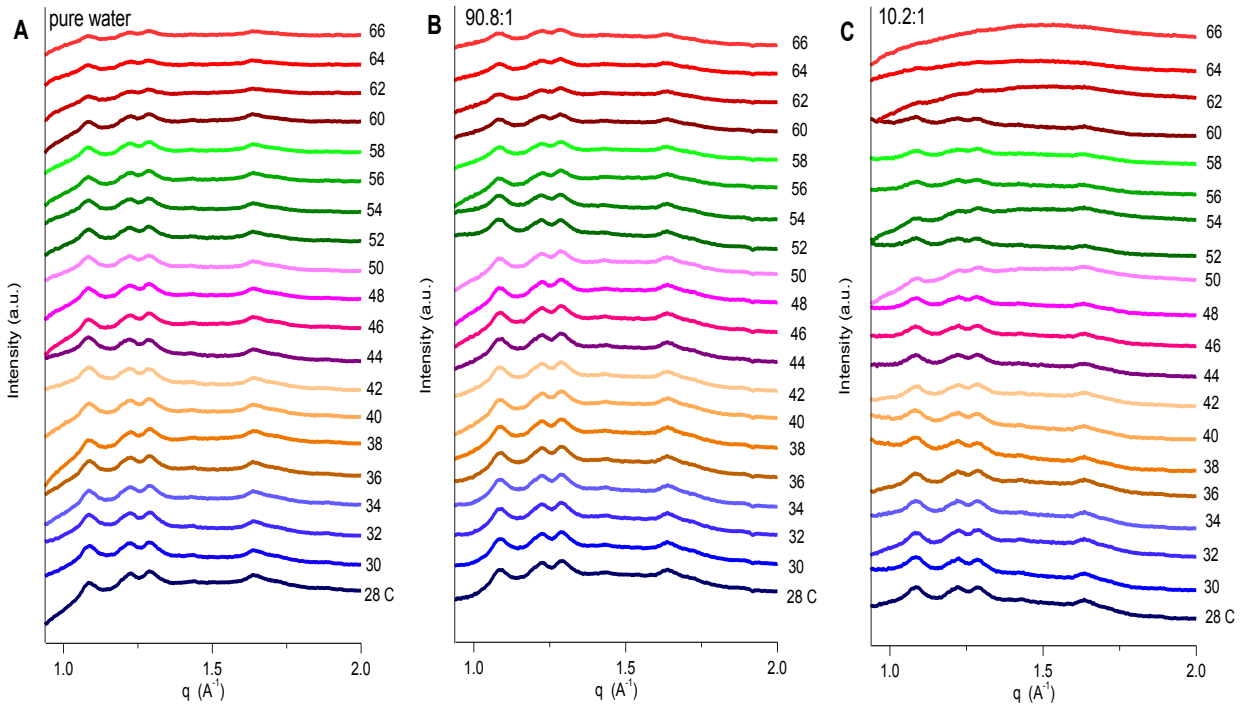

Fig. 2 Temperature-resolved WAXS patterns for the starch in pure water (A) and 90.8:1 (B) and 10.2:1 (C) mol/mol water:[C_2mim][OAc] solutions.

3.3. Temperature-resolved small-angle X-ray scattering (SAXS) analysis

The temperature resolved SAXS patterns (contour maps) and their surface patterns for the starch in pure water and 90.8:1 and 10.2:1 mol/mol solutions are shown in Fig. 3. A typical SAXS peak could be observed at q of 0.06 to 0.07 $Å^{-1}$, corresponding to the semi-crystalline lamellar structure of starch. The change of this scattering peak can indicate the disruption of semi-crystalline lamellae during thermal treatment.[48, 52, 53] Fig. 3A and 3B show that, for the starch in pure water, heating resulted in reduction in peak region intensity, especially steep decreases at about 47 °C and 61 °C, in the sub-melting temperature range ($< T_o$). In contrast, for the starch in the 90.8:1 mol/mol solution, the peak region intensity decreased more gradually from 45 °C, before T_o (Fig. 3C and 3D). When the concentration of $[C_2mim][OAc]$ was increased to 50 wt% (10.2:1 mol/mol), the transition in the sub-melting temperature range ($< T_o$) occurred at largely reduced temperature (from 39 °C), as compared to those with pure water, with the peak becoming negligible at 66 °C (Fig. 3E and 3F).

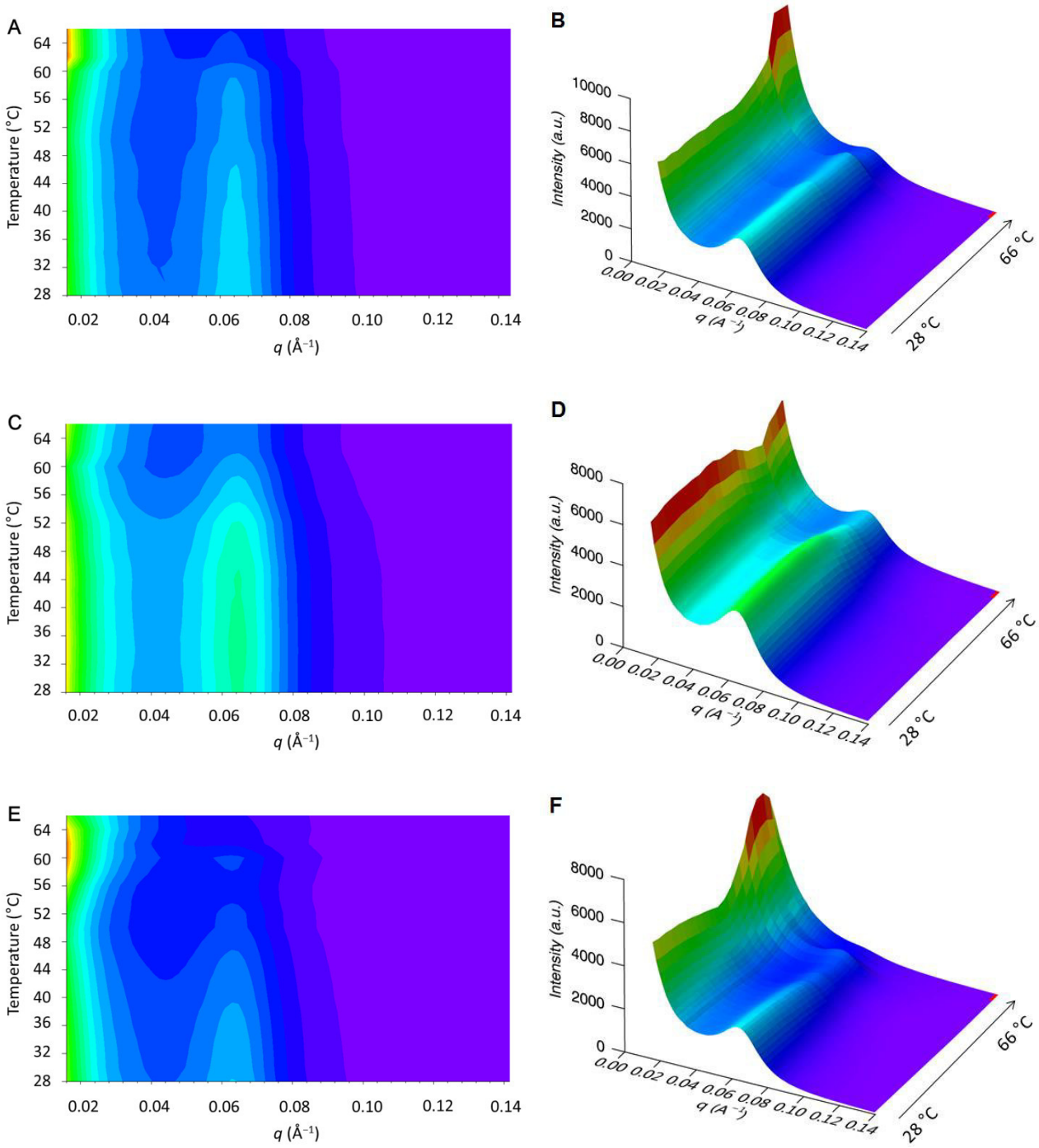

Fig. 3 Temperature-resolved SAXS patterns (contour maps) (A, C, and E) and their surfaces (B, D, and F) for the starch in pure water (A and B) and 90.8:1 (C and D) and 10.2:1 mol/mol (E and F) water:[C_2mim][OAc] solutions . The brighter color indicates stronger SAXS intensity.

Fig. 4 further illustrates the changes in SAXS peak area with increase in temperature. The peak area indicates the degree of lamellae ordering.[54] For the starch in pure water or the 90.8:1 mol/mol

solution, the peak area formed a plateau region before decreasing, whereas it gradually decreased from the start (28 °C) for the starch in the 10.2:1 mol/mol solution. Moreover, the peak area was even higher in the 90.8:1 mol/mol solution than in pure water, whereas it was significantly weakened by the 10.2:1 mol/mol solution. All these results clearly demonstrate that, even in the sub-melting temperature range ($< T_o$), adding a small amount (*e.g.,* 10 wt%) of [C_2mim][OAc] to water could make the structural disorganization of starch more difficult (apparently by perfecting the structural definition), whereas the disordering of starch lamellae could be greatly facilitated by the 10.2:1 mol/mol solution.

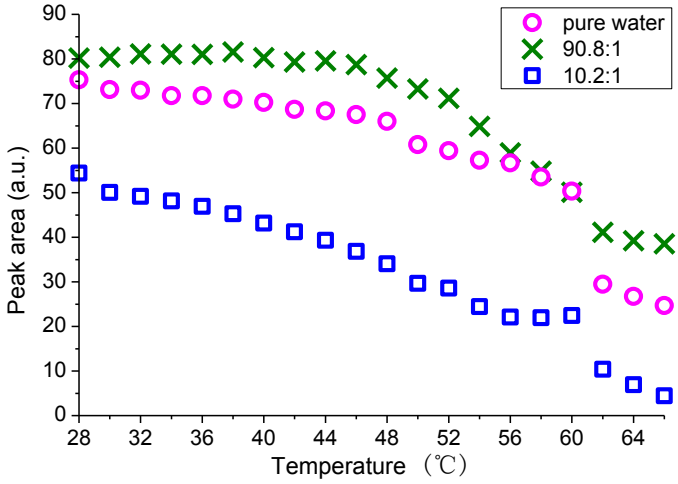

Fig. 4 Changes in SAXS peak area as a function of temperature for starch in pure water (pink circles) and 90.8:1 (green crosses) and 10.2:1 mol/mol (blue squares) water:[C_2mim][OAc] solutions.

The changes in α (the power-law exponent in Eq. (1)) for the starch in different solutions are shown in Fig. 5A. α ranged from 1 to 3 for the starch in three solutions at 28 °C. α values in this range are normally associated with a mass fractal (self-similar) structure and/or a lamellar structure.[55] Before T_o, the lamellar structure should be mostly retained and thus its contribution to α should be the same.[55] Therefore, α was mainly associated with the formation of fractal structure here.

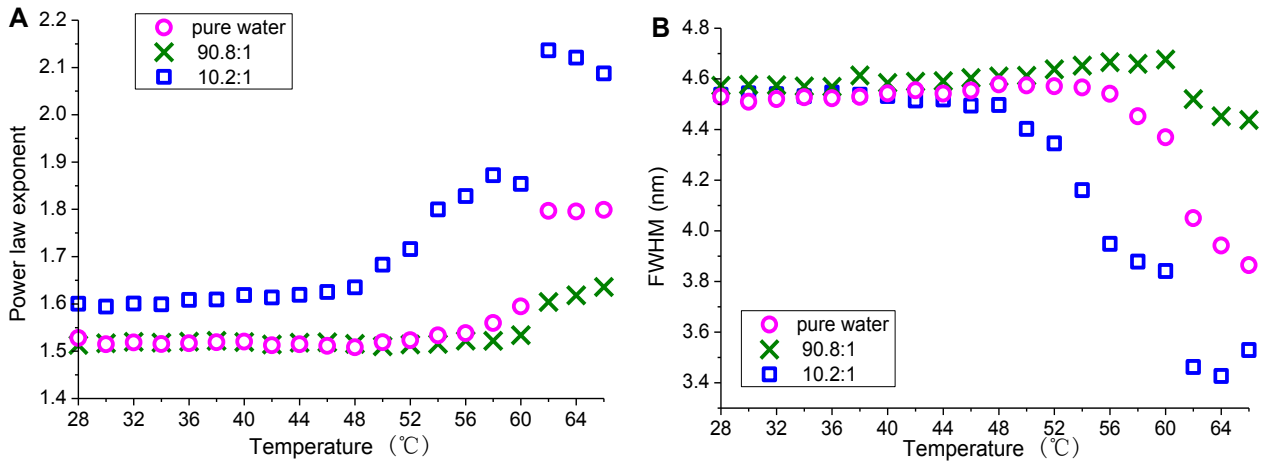

Fig. 5 Changes in the power law exponent (α) and peak width at half-maximum in the real space (FWHM) as a function of temperature for the starch in pure water (pink circles) and 90.8:1 (green crosses) and 10.2:1 mol/mol (blue squares) water:[C_2mim][OAc] solutions.

With increased temperature, the starch in pure water displayed an unchanged α value until 52 °C; then increased, presumably due to the appearance of a mass fractal structure. This is also supported by the observation in Fig. 3B: when the temperature was higher than 52 °C, the scattering at q values lower than the peak position showed gradual increase with increased temperature, indicating the formation of a larger-scale structure (than the lamellae). Meanwhile, the scattering peak showed reduced intensity, suggesting the disordering of the semi-crystalline lamellae. Thus, it is reasonable to suppose, even in the sub-melting temperature range ($< T_o$), water could partially disorder the semi-crystalline lamellae, phasing out starch molecules to form a fractal gel on a larger scale.

Compared with pure water, 10 wt% of [C_2mim][OAc] in water postponed the changes in α, whereas a higher [C_2mim][OAc] concentration reduced the onset temperature for the increase in α, and generated more significant increases in α. Specifically α started to increase when the temperatures were 60 °C and 48 °C for the 90.8:1 and 10.2:1 mol/mol solutions, respectively. The difference in the onset temperature for α for the different solutions is consistent with the results discussed previously — that is, compared with pure water, the 90.8:1 mol/mol solution could make

the structure more resistant to change but the 10.2:1 mol/mol solution could greatly expedite the structural change.

Fig. 5B shows the plots of FWHM against temperature for different samples. The FWHM represents the lamellar thickness distribution.[46] Whilst both pure water and the 90.8:1 mol/mol solution moderately widened the FWHM of starch with the temperature increased up to 52 °C and 60 °C, respectively, the 10.2:1 mol/mol solution slightly reduced the value at temperatures up to 48 °C. The relatively stable FWHM values below the FWHM onset temperatures probably indicate an overall thickness increase of the semi-crystalline lamellae for the starch in all three solutions. Once the temperature exceeded the FWHM onset point, the decrease in FWHM should be due to further increase in thickness of mostly the relatively smaller lamellae. This phenomenon was more intensive for the starch in the 10.2:1 mol/mol solution.

It is noteworthy that for the starch in different solutions, the onset temperature for the FWHM to decrease was the same as that for α to increase (see Fig. 5A), indicating the co-occurrence of the change in lamellar size distribution and the formation of mass fractal gel after the onset temperature. In addition, both α and FWHM showed a large shift from 60 °C to 62 °C (see Fig. 5), especially for the starch in pure water and the 10.2:1 mol/mol solution, suggesting dramatic changes in the lamellar size distribution and the formation of mass fractal gel structure at a specific temperature. This could be verified by a sharp decrease in the peak intensity and area and a steep increase in the scattering at q values lower than the peak position at ca. 60 °C (see Fig. 3 and Fig. 4). For further understanding the solvent effects of water:[C_2mim][OAc] solutions on the starch, the statistically average parameters of the semi-crystalline lamellae were also computed (see Fig. 6), including the average thicknesses of the semi-crystalline (d), crystalline (d_c) and amorphous (d_a) lamellae. Fig. 6A and B shows that, both d and d_c kept constant initially and then simultaneously started to increase at 48 °C, 54 °C, and 42 °C for the starch in pure water and the 90.8:1 and 10.2:1 mol/mol solutions, respectively. All these temperatures were lower than the corresponding onset temperatures for α or

FWHM (see Fig. 5A and 5B). Additionally, Fig. 6C shows that for the starch in the 10.2:1 mol/mol solution, d_a remained almost unchanged until 48 °C, which was the same as the α/FWHM onset temperature; but with pure water and the 90.8:1 mol/mol solution, the onset temperatures for d_a to decrease were 60 °C and 66 °C respectively, which were higher than the α/FWHM onset temperatures (52 °C and 60 °C respectively).

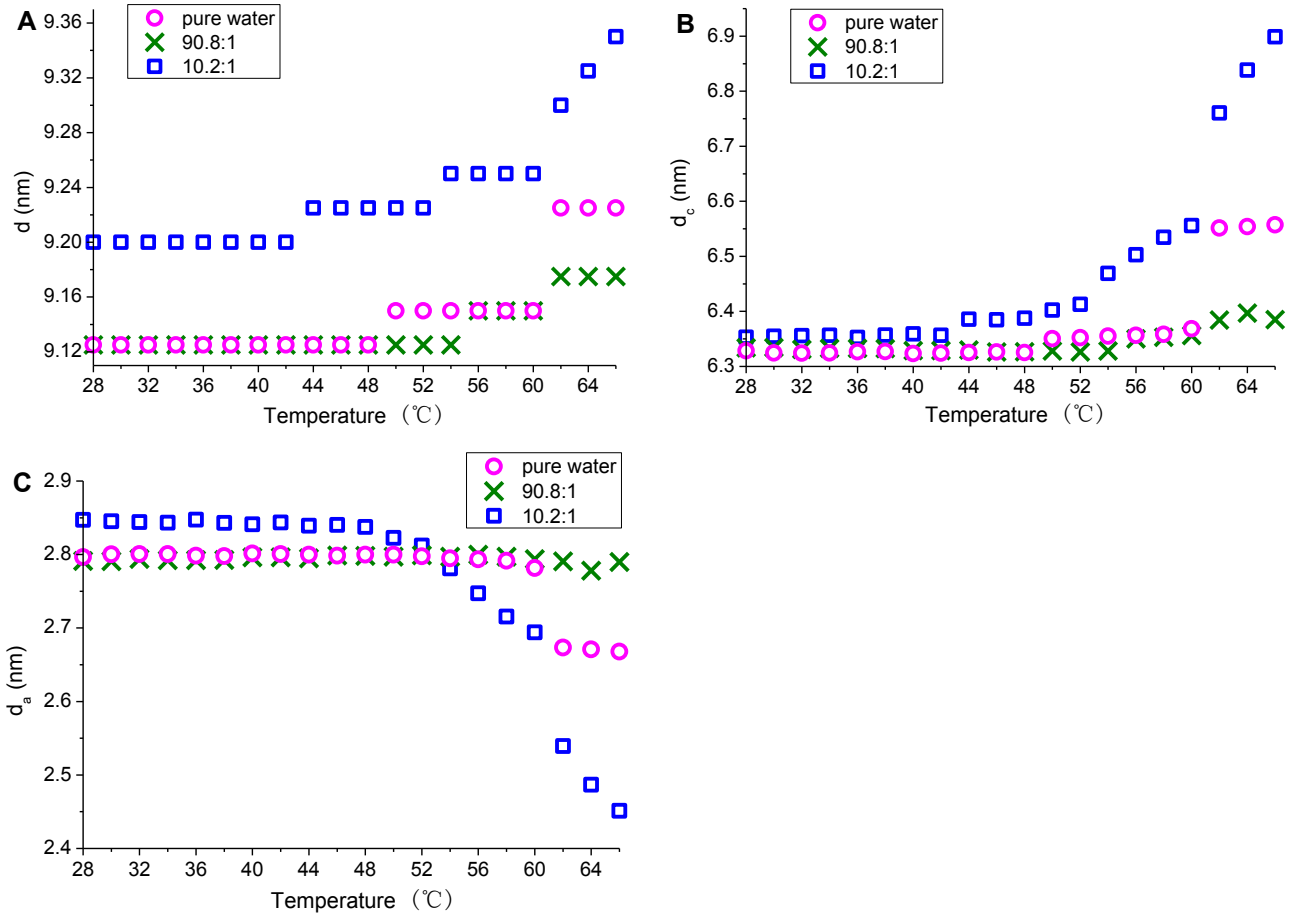

Fig. 6 Changes in lamellar parameters as a function of temperature for starch in pure water (pink circles) and in 90.8:1 (green crosses) and 10.2:1 mol/mol (blue squares) water:[C_2mim][OAc] solutions. Values d, d_a, and d_c are the average thicknesses of the semi-crystalline, crystalline and amorphous lamellae, respectively.

These results of average thicknesses, along with the previous discussion on α/FWHM, can further clarify the changes of starch lamellar structure (see Fig. 7): a) initially, all three solutions tended to increase the thickness of the semi-crystalline lamellae by increasing the thickness of the crystalline lamellae rather than that of the amorphous lamellae; and until the α/FWHM onset temperature, this increase was an overall thickness increase of all the semi-crystalline lamellae (as seen by the increased d and d_c but stable d_a, and the relatively stable FWHM) (from I to II in Fig. 7); b) from the α/FWHM onset temperature to the d_a onset temperature, there was a further increase in the thickness of especially the relatively smaller lamellae (as seen by the decrease in FWHM) (from II to III in Fig. 7); c) after the d_a onset temperature, the amorphous lamellae started to decrease probably due to the out-phasing of starch molecules from them (from III to IV in Fig. 7). In particular, for the starch in the 10.2:1 mol/mol solution, the α/FWHM onset temperature was the same as the d_a onset temperature, indicating that the corrosion of the amorphous lamellae immediately causes a decrease in the amorphous lamellar thickness. This, again, demonstrates that the 10.2:1 mol/mol solution could cause more drastic changes to the starch.

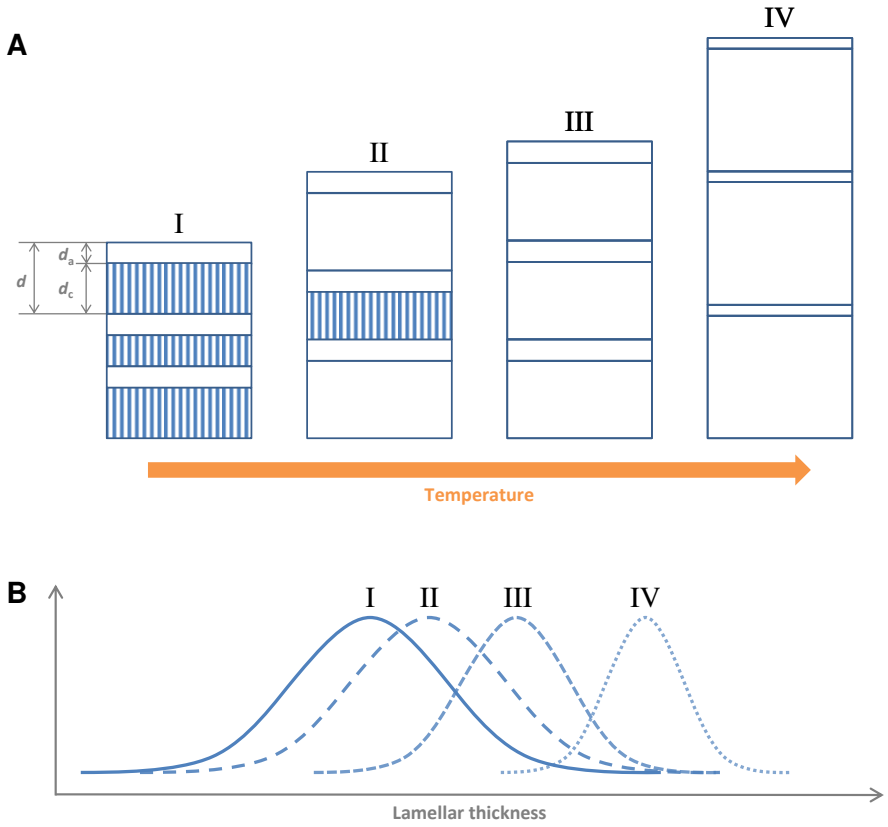

Fig. 7 Schematic representations of the changes in lamellar thickness (A) and its distribution (B).

3.4. Wide- and small-angle X-ray scattering (WAXS/SAXS) analysis for gel features

To further investigate the solvent effects of different water:[C_2mim][OAc] solutions on the destructuration of starch, the WAXS and SAXS patterns of the starch in these solutions were recorded at 76 °C (Fig. 8A), higher than the T_o values. As shown in the WAXS results in Fig. 8A (compared with Fig. 2), the starch should predominantly display a gel feature at 76 °C. While both pure water and the 10.2:1 mol/mol solution made the starch crystallites undetectable, the starch in the 90.8:1 mol/mol solution still displayed weak residual peaks (indicated by the arrows in Fig. 8A). In addition, for the starch in both pure water and the 90.8:1 mol/mol solution, a peak could be seen on the SAXS patterns (Fig. 8B and 8C), suggesting that 76 °C was not high enough to destroy the starch lamellae in the pure water and the 90.8:1 mol/mol solution. Nevertheless, the 10.2:1 mol/mol solution could fully melt the semi-crystalline lamellae at 76 °C (Fig. 8D).

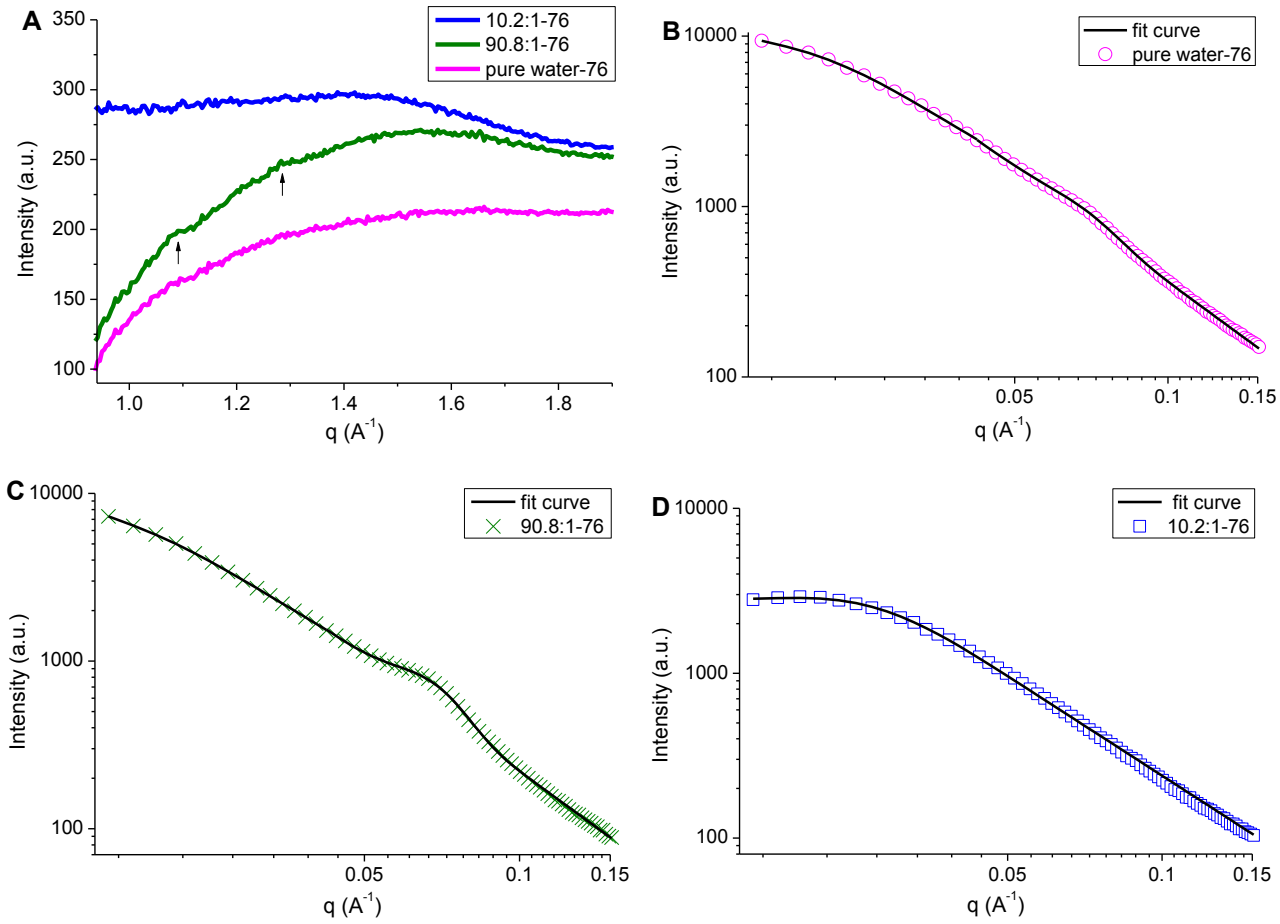

Fig. 8 WAXS patters (A) and SAXS patterns (B, C, and D, respectively) with their fit curves for starch at 76 °C in pure water (pink) and in 90.8:1 (green) and 10.2:1 mol/mol (blue) water:[C_2mim][OAc] solutions.

A more apparent inflection of the SAXS pattern at low q values was observed for the starch in the 10.2:1 mol/mol solution than those for the other two samples (pure water and the 90.8:1 mol/mol solution) (Fig. 8). This inflection correlates to the Guinier scattering behavior (*i.e.*, a structure with a certain radius of gyration (R_g)).[56] R_g actually corresponds to the size of fractal aggregates (gel).[57] Table 1 summarizes the fitted R_g and other SAXS parameters for the starch in all three solutions at 76 °C. The starch showed power-law exponents (δ, calculated from Eq. (4) based on the range of q < 0.045 Å^{-1}; and α_1, from Eq. (1) based on the range of 0.045 < q < 0.15 Å^{-1}) values between 1.6 and

2.3, indicating the mass fractal structure of starch gel.[58] The fractal gel in the solutions had R_g values in the order of 10.2:1 mol/mol solution < pure water < 90.8:1 mol/mol solution at 76 °C. This indicates that the 10.2:1 mol/mol solution could more effectively transform the starch into fractal gel with smaller R_g, than either pure water or the 90.8:1 mol/mol solution. This also corresponds to the effectiveness of the solutions to destructure the starch, as discussed before.

Table 1 SAXS parameters of the starch samples in pure water and 90.8:1 and 10.2:1 (mol/mol) water:[C_2mim][OAc] solutions at different temperatures. (δ is calculated from Eq. (4) based on the range of q < 0.045 Å^{-1}; and α_1 from Eq. (1) based on the range of 0.045 < q < 0.15 Å^{-1})

		Pure Water	90.8:1	10.2:1
62 °C	R_g (Å)	–	–	250.90 ± 1.85[a]
	δ	–	–	1.96 ± 0.03
	α_1	–	–	2.14± 0.05
64 °C	R_g (Å)	–	–	214.74 ± 7.39
	δ	–	–	1.86 ± 0.24
	α_1	–	–	2.12± 0.03
66 °C	R_g (Å)	–	–	184.00 ± 5.52
	δ	–	–	1.72 ± 0.03
	α_1	–	–	2.09± 0.02
74 °C	R_g (Å)	212.85 ± 6.96	252.89 ± 6.96	140.83 ± 6.96
	δ	1.59 ± 0.02	1.81 ± 0.03	1.62 ± 0.01
	α_1	2.14± 0.03	2.11± 0.09	2.02± 0.03
76 °C	R_g (Å)	177.33 ± 3.54	198.47 ± 4.78	140.59 ± 1.84
	δ	1.79 ± 0.03	1.85 ± 0.02	1.64 ± 0.04
	α_1	2.22 ± 0.02	2.24 ± 0.03	2.05 ± 0.02

[a] Standard error

Table 1 also shows the changes in R_g for the starch in the different solutions with the increased temperature. The selected temperatures were those when evident changes can be observed from the temperature-resolved WAXS results. For the starch in pure water or the 90.8:1 mol/mol solution, R_g was reduced with the temperature increased from 74 °C to 76 °C. This suggests that the mass fractal gel firstly formed on a large scale and then the gel size could be reduced at a higher temperature. This was more evident for the starch in the 10.2:1 mol/mol solution, as R_g was gradually reduced when the temperature increased from 62 °C to 74 °C, indicating increased homogeneity of the starch–water–IL system. However, further increase in temperature to 76 °C did not change the gel size further. This means there was a stable size of fractal gel that could be maintained with increased temperature.

3.5. Attenuated total reflectance–Fourier transform infrared (ATR-FTIR) spectroscopy for molecular interactions

The potential of ILs as solvents for naturally-derived polymers such as cellulose has been widely reported.[59-62] It has been suggested that basic IL anions (chloride,[59, 63] hydroxide,[64] formate[65]), acting as proton acceptors, would efficiently promote cellulose dissolution by forming hydrogen bonds (H-bonds or H-bonding) with cellulose hydroxyl groups. Both starch and cellulose are polysaccharides consisting of D-glucose units, referred to as homoglucan or glucopyranose. The main difference between the two is that the units of starch are mostly linked by α-1,4-glycosidic bonds, while those of cellulose are connected by β-1,4 glycosidic bonds while the number of hydroxyls is the same in both polymers suggesting that the solvent effects of water–IL solutions on starch are also governed by the H-bonding interactions between water and acetate anion. Water has been shown to affect the dissolution behavior of [C_2mim][OAc], even at low concentrations. When IL is mixed with water, different types of interactions between water and the IL ions arise that have been studied *via* theoretical calculations[66] and experimentally with physical property measurements[67] and spectroscopic studies[68].

It was found that in water:[C_2mim][OAc] solutions, there are three main types of interactions. First, there is a reaction of water with the $[OAc]^-$ anion (although the equilibrium is greatly shifted to the acetate because of the pKa difference between water and HOAc, 10.22) and water–IL solutions are basic, with pH values of 12.5 in 10 wt% water solutions (*ca.* 1:1 mol/mol) to 10.9 at 25 wt% water (*ca.* 3:1 mol/mol water:[C_2mim][OAc]).[69] Second, there is a strong hydrogen-bond network between water and $[OAc]^-$ anions, predominating over the water–water and IL–IL interactions at most water concentrations.[66] At low water concentrations (water:[C_2mim][OAc] *ca.* 1:8 mol/mol), calculations suggested that each water molecule is coordinated by two $[OAc]^-$ anions and each $[OAc]^-$ anion is solvated by 0.25 water molecules, whereas at high water concentration (water:[C_2mim][OAc] 1:1 mol/mol), water and the $[OAc]^-$ anion form an "extended hydrogen-bonding network" with each water molecule still coordinated by two $[OAc]^-$ anions but each $[OAc]^-$ anion coordinated by two water molecules.[66] At yet higher water concentrations, the IL as a whole still behaves as a continuous phase and water molecules fill in the empty space between the IL ions. Recent NMR spin relaxation and exchange spectroscopy studies suggested a third type of interaction, a proton exchange between H-2 of the imidazolium cation and water molecules, through the initial formation of carbene in the basic environment.[68] While there is a complex dependence on the concentration of the solution, at 1:1 mol/mol concentration there is fast proton exchange of H-2 and water, as well as an extended water:[C_2mim][OAc] hydrogen bonded network.

In our investigation of starch dissolution in water:[C_2mim][OAc] solutions, we conducted FTIR studies to probe the effects of these possible interactions on the $[OAc]^-$ anion. As seen in Fig. 9A, the $[OAc]^-$ anion in the pure IL had two apparent IR absorption peaks at 1380 cm^{-1} and at 1580 cm^{-1} ascribed to the symmetric and asymmetric O–C–O stretches, respectively.[70] With addition of water, the peak at 1380 cm^{-1} shifted to higher frequency of 1413 cm^{-1}, while the peak 1580 cm^{-1} shifted to lower frequency of 1567 cm^{-1}. The magnitude of these shifts increased with increasing amounts of water demonstrating the interaction between the IL and water. The same direction and magnitude of

shifts for these O–C–O stretching bands was observed for the $[OAc]^-$ anion in [Na][OAc] when dissolved in water (Fig. 9B). Additionally, when $[C_2mim][OAc]$ was added to water, the IR absorption band of pure water at *ca.* 3400 cm^{-1} (the hydroxyl stretch band) showed an apparent reduction in intensity, the more so the more $[C_2mim][OAc]$ was present in a solution (Fig. 9E), possibly due to lower water content. When the solution had a relatively large amount of $[C_2mim][OAc]$ added (23.6:1 or 10.2:1 water:IL mol/mol), a second peak at *ca*. 3160 cm^{-1} appeared and there were clearly two types of –OH stretches present.

The addition of starch to pure water decreased water hydroxyl stretch (Fig. 9E) indicating solvation of starch with abundant water molecules. The addition of starch to the water:$[C_2mim][OAc]$ solutions when the amount of water was high (the 90.8:1 or 24.3:1 mol/mol water:$[C_2mim][OAc]$ solutions) did not have a noticeable effect on the number, position, or intensity of the acetate or hydroxyl stretches (Fig. 9C, D and E); we believe there was enough water to both solvate starch and interact with $[OAc]^-$ anion; consequently, $[OAc]^-$ anion had little chance to effectively interact with the starch molecules. Contrarily, when the amount of water is low (the 10.2:1 mol/mol water:$[C_2mim][OAc]$ solution), slight reduction in intensity and small shift of acetate stretches was observed with addition of starch (Fig. 9C, D) indicating decrease of $[C_2mim][[OAc]$–water interaction and the ability of the acetate to still interact with the starch. This is in accordance with a previous study revealing that the kosmotropic effect of $[OAc]^-$ for interaction with a polyol hydrogen-bond network could be decreased when the anion is hydrated.[18]

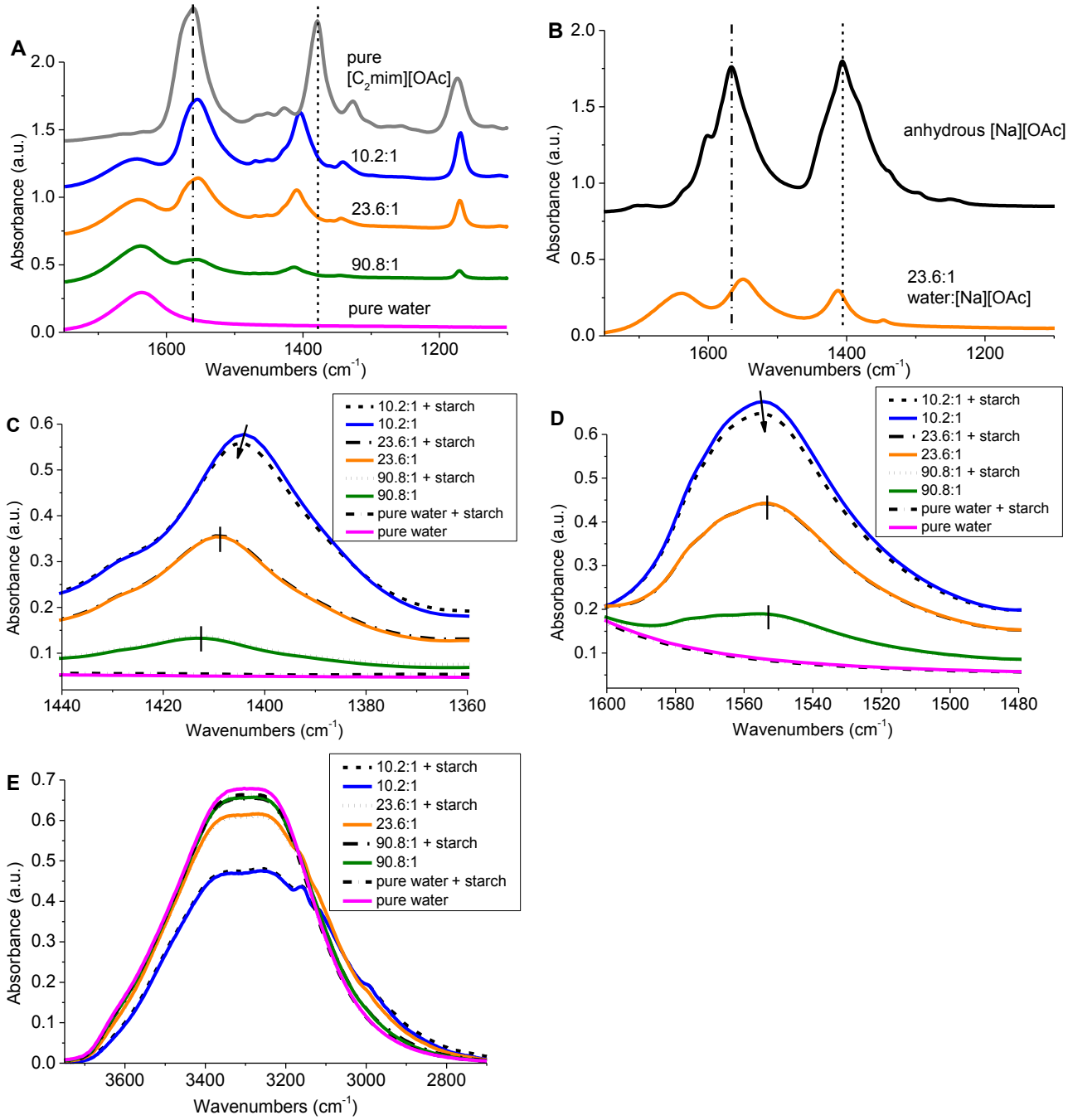

Fig. 9 ATR-FTIR spectra of pure water and water:[C_2mim][OAc] solutions of different mole ratios (A) (pure water, pink; 90.8:1 mol/mol, green; 23.6:1, orange; 10.2:1, blue; pure [C_2mim][OAc], grey); anhydrous [Na][OAc] and 23.6:1 (mol/mol) water:[Na][OAc] solution (B); and pure water and water:[C_2mim][OAc] solutions containing 10 wt% starch after thermal treatment at 76 °C for 30 min (B, C and D for different wavenumber ranges).

4. Conclusions

Water–IL solutions have been demonstrated to be effective at increasing the destructuration of native starch. This provides a way to process starch with reduced energy consumption, and also a simple method to tailor the starch products with controlled structures. For these purposes, this study explored the solvent effects of water:[C_2mim][OAc] solutions and the related mechanism.

In water:[C_2mim][OAc] solutions, thermal treatment would destructurize starch by increasing the thickness of crystalline lamellae, but reducing that of amorphous lamellae leading to out-phasing of starch molecules to form a mass fractal at a larger scale (than the scale of lamellae). As temperature further increased, the radius of gyration for fractal aggregates (gel) was reduced to a stable value, allowing an increase in homogeneity of the starch–water–IL system. Nevertheless, the solutions containing different amounts of [C_2mim][OAc] showed different solvent effects on the structural disorganization of starch, due to changes in the H-bonding interactions between water and acetate anion.

The ionic liquid solutions only showed differences in the FTIR when starch was added when the concentration of water was very low which we attribute to the ability of the acetate to still interact with the starch because there was not enough water to solvate both the starch and the acetate; this solution was slightly more effective in changing the starch structure. In the high water concentration we had no differences in the IR before or after starch was added because there was enough water to completely solvate both the starch and the acetate, preventing any interaction between them. This in turn made the solution less effective in changing the starch structure and the starch transition temperature higher.

The results from present work should be of value in rational development of new green methods based on water–IL solution to process semi-crystalline natural polymers (*e.g.*, dextrin, cellulose, and xylan), other than starch, containing hydroxyls (involving strong inter- and intra-molecular hydrogen bonding) for industrial applications.

Acknowledgements

The research leading to these results has received funding from the Australian Research Council (ARC) under the Discovery Project 120100344. This research was undertaken on the SAXS/WAXS beamline at the Australian Synchrotron, Victoria, Australia. B. Zhang also would like to thank the China Scholarship Council (CSC) for providing research funding for his visiting studies at The University of Queensland (UQ) as part of his Ph.D. work.

Notes and references

1. P. Gallezot, *Green Chem.*, 2007, 9, 295-302.
2. A. Gandini, *Green Chem.*, 2011, 13, 1061-1083.
3. L. Yu, K. Dean and L. Li, *Prog. Polym. Sci.*, 2006, 31, 576-602.
4. R. L. Shogren, G. F. Fanta and W. M. Doane, *Starch/Stärke*, 1993, 45, 276-280.
5. H. Liu, F. Xie, L. Yu, L. Chen and L. Li, *Prog. Polym. Sci.*, 2009, 34, 1348-1368.
6. F. Xie, P. J. Halley and L. Avérous, *Prog. Polym. Sci.*, 2012, 37, 595-623.
7. F. Xie, P. Liu and L. Yu, in *Starch Polymers: From Genetic Engineering to Green Applications*, eds. P. J. Halley and L. R. Avérous, Elsevier, Amsterdam, Netherlands, 1st edn., 2014, DOI: 10.1016/B978-0-444-53730-0.00024-5, ch. 10, pp. 257-289.
8. S. Pérez, P. M. Baldwin and D. J. Gallant, in *Starch (Third Edition)*, eds. B. James and W. Roy, Academic Press, San Diego, 2009, pp. 149-192.
9. J.-l. Jane, in *Starch (Third Edition)*, eds. B. James and W. Roy, Academic Press, San Diego, 2009, pp. 193-236.
10. S. Pérez and E. Bertoft, *Starch/Stärke*, 2010, 62, 389-420.
11. Z.-q. Fu, L.-j. Wang, D. Li, Q. Wei and B. Adhikari, *Carbohydr. Polym.*, 2011, 86, 202-207.
12. M. R. Debet and M. J. Gidley, *J. Agric. Food Chem.*, 2007, 55, 4752-4760.
13. D. H. John and D. R. Robin, in *Ionic Liquids*, American Chemical Society, 2002, vol. 818, ch. 1, pp. 2-14.
14. K. Lappalainen, J. Kärkkäinen and M. Lajunen, *Carbohydr. Polym.*, 2013, 93, 89-94.

15. R. P. Swatloski, S. K. Spear, J. D. Holbrey and R. D. Rogers, *J. Am. Chem. Soc.*, 2002, 124, 4974-4975.

16. S. Tan and D. MacFarlane, in *Ionic Liquids*, ed. B. Kirchner, Springer Berlin Heidelberg, 2010, vol. 290, ch. 35, pp. 311-339.

17. A. Pinkert, K. N. Marsh, S. Pang and M. P. Staiger, *Chem. Rev.*, 2009, 109, 6712-6728.

18. Z. Papanyan, C. Roth, K. Wittler, S. Reimann and R. Ludwig, *ChemPhysChem*, 2013, 14, 3667-3671.

19. A. Biswas, R. L. Shogren, D. G. Stevenson, J. L. Willett and P. K. Bhowmik, *Carbohydr. Polym.*, 2006, 66, 546-550.

20. O. A. El Seoud, A. Koschella, L. C. Fidale, S. Dorn and T. Heinze, *Biomacromolecules*, 2007, 8, 2629-2647.

21. M. E. Zakrzewska, E. Bogel-Łukasik and R. Bogel-Łukasik, *Energy Fuels*, 2010, 24, 737-745.

22. K. Wilpiszewska and T. Spychaj, *Carbohydr. Polym.*, 2011, 86, 424-428.

23. N. Wang, X. Zhang, X. Wang and H. Liu, *Macromol. Res.*, 2009, 17, 285-288.

24. N. Wang, X. Zhang, H. Liu and B. He, *Carbohydr. Polym.*, 2009, 76, 482-484.

25. N. Wang, X. Zhang, H. Liu and N. Han, *Polym. Polym. Compos.*, 2010, 18, 53-58.

26. S. Ramesh, C.-W. Liew and A. K. Arof, *J. Non-Cryst. Solids*, 2011, 357, 3654-3660.

27. S. Ramesh, R. Shanti, E. Morris and R. Durairaj, *Mater. Res. Innovations*, 2011, 15, s8.

28. C.-W. Liew, S. Ramesh, K. Ramesh and A. Arof, *J. Solid State Electrochem.*, 2012, 16, 1869-1875.

29. S. Ramesh, R. Shanti and E. Morris, *Solid State Sci.*, 2012, 14, 182-186.

30. D. G. Stevenson, A. Biswas, J.-l. Jane and G. E. Inglett, *Carbohydr. Polym.*, 2007, 67, 21-31.

31. J. Kärkkäinen, K. Lappalainen, P. Joensuu and M. Lajunen, *Carbohydr. Polym.*, 2011, 84, 509-516.

32. S. Mateyawa, D. F. Xie, R. W. Truss, P. J. Halley, T. M. Nicholson, J. L. Shamshina, R. D. Rogers, M. W. Boehm and T. McNally, *Carbohydr. Polym.*, 2013, 94, 520-530.

33. W. Liu and T. Budtova, *Carbohydr. Polym.*, 2013, 93, 199-206.

34. L. S. Sciarini, A. Rolland-Sabate, S. Guilois, P. Decaen, E. Leroy and P. Le Bail, *Green Chem.*, 2015, 17, 291-299.

35. A. Brandt, J. Grasvik, J. P. Hallett and T. Welton, *Green Chem.*, 2013, 15, 550-583.

36. A. Brandt, J. P. Hallett, D. J. Leak, R. J. Murphy and T. Welton, *Green Chem.*, 2010, 12, 672-679.

37. A. Brandt, J. K. Erickson, J. P. Hallett, R. J. Murphy, A. Potthast, M. J. Ray, T. Rosenau, M. Schrems and T. Welton, *Green Chem.*, 2012, 14, 1079-1085.

38. A. Brandt, M. J. Ray, T. Q. To, D. J. Leak, R. J. Murphy and T. Welton, *Green Chem.*, 2011, 13, 2489-2499.

39. S. Xia, G. A. Baker, H. Li, S. Ravula and H. Zhao, *RSC Advances*, 2014, 4, 10586-10596.

40. J. Lupoi, S. Singh, B. Simmons and R. Henry, *Bioenerg. Res.*, 2014, 7, 1-23.

41. G. Cheng, X. Zhang, B. Simmons and S. Singh, *Energy & Environmental Science*, 2015, 8, 436-455.

42. H. Wang, G. Gurau, S. V. Pingali, H. M. O'Neill, B. R. Evans, V. S. Urban, W. T. Heller and R. D. Rogers, *ACS Sustainable Chemistry & Engineering*, 2014, 2, 1264-1269.

43. I. Tan, B. M. Flanagan, P. J. Halley, A. K. Whittaker and M. J. Gidley, *Biomacromolecules*, 2007, 8, 885-891.

44. F. Xie, B. M. Flanagan, M. Li, P. Sangwan, R. W. Truss, P. J. Halley, E. V. Strounina, A. K. Whittaker, M. J. Gidley and K. M. Dean, *Carbohydr. Polym.*, 2014.

45. J. Blazek and E. P. Gilbert, *Biomacromolecules*, 2010, 11, 3275-3289.

46. T. Witt, J. Doutch, E. P. Gilbert and R. G. Gilbert, *Biomacromolecules*, 2012, 13, 4273-4282.

47. A. Lopez-Rubio, B. M. Flanagan, E. P. Gilbert and M. J. Gidley, *Biopolymers*, 2008, 89, 761-768.

48. B. J. Zhang, X. X. Li, J. Liu, F. W. Xie and L. Chen, *Food Hydrocolloids*, 2013, 31, 68-73.

49. B. J. Zhang, S. X. Xiong, X. X. Li, L. Li, F. W. Xie and L. Chen, *Food Hydrocolloids*, 2014, 37, 69-76.

50. A. Lopez-Rubio, B. M. Flanagan, E. P. Gilbert and M. J. Gidley, *Biopolymers*, 2008, 89, 761-768.

51. S. Perez and E. Bertoft, *Starch-Starke*, 2010, 62, 389-420.

52. B. J. Zhang, Y. Zhao, X. X. Li, L. Li, F. W. Xie and L. Chen, *Food Hydrocolloids*, 2014, 35, 700-709.

53. D. J. Gallant, B. Bouchet and P. M. Baldwin, *Carbohydr. Polym.*, 1997, 32, 177-191.

54. S. Pikus, *Fibres Text East Eur*, 2005, 13, 82-86.

55. J. Doutch and E. P. Gilbert, *Carbohydr Polym*, 2013, 91, 444-451.

56. G. Beaucage, *Physical Review E*, 2004, 70, 031401.

57. J. Doutch, M. Bason, F. Franceschini, K. James, D. Clowes and E. P. Gilbert, *Carbohydr. Polym.*, 2012, 88, 1061-1071.

58. T. Suzuki, A. Chiba and T. Yarno, *Carbohydr. Polym.*, 1997, 34, 357-363.

59. R. C. Remsing, R. P. Swatloski, R. D. Rogers and G. Moyna, *Chemical Communications*, 2006, 1271-1273.

60. Y. Fukaya, K. Hayashi, M. Wada and H. Ohno, *Green Chem.*, 2008, 10, 44-46.

61. H. Wang, G. Gurau and R. D. Rogers, *Chem. Soc. Rev.*, 2012, 41, 1519-1537.

62. N. Sun, H. Rodriguez, M. Rahman and R. D. Rogers, *Chem. Commun.*, 2011, 47, 1405-1421.

63. C. Zhang, R. Liu, J. Xiang, H. Kang, Z. Liu and Y. Huang, *The Journal of Physical Chemistry B*, 2014.

64. M. Abe, Y. Fukaya and H. Ohno, *Chemical Communications*, 2012, 48, 1808-1810.

65. Y. Fukaya, A. Sugimoto and H. Ohno, *Biomacromolecules*, 2006, 7, 3295-3297.

66. W. Shi, K. Damodaran, H. B. Nulwala and D. R. Luebke, *Phys. Chem. Chem. Phys.*, 2012, 14, 15897-15908.

67. K. Le, R. Sescousse and T. Budtova, *Cellulose*, 2012, 19, 45-54.

68. J. J. Allen, S. R. Bowser and K. Damodaran, *Phys. Chem. Chem. Phys.*, 2014, 16, 8078-8085.

69. C. A. Ober and R. B. Gupta, *Ind. Eng. Chem. Res.*, 2012, 51, 2524-2530.

70. J. M. Delgado, A. Rodes and J. M. Orts, *The Journal of Physical Chemistry C*, 2007, 111, 14476-14483.

Table S1 The formulations, in mass and in mole, used in the experimental work

Mass ratio			Mole ratio		
Water	$[C_2mim][OAc]$	Starch	Water	$[C_2mim][OAc]$	Starch –OH
10	0	1	100.77	0	2.91
9	1	1	90.83	1	2.91
7	3	1	23.65	1	0.97
5	5	1	10.21	1	0.58

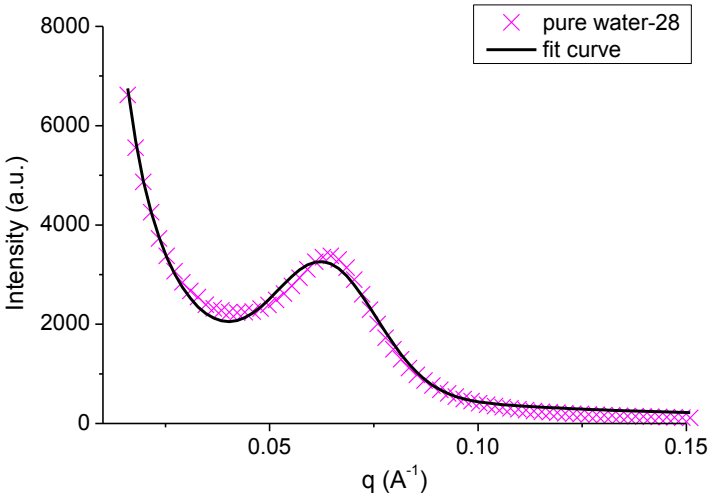

Fig. S1 SAXS patterns and their fit curves of the starch samples at 28 °C in pure water.

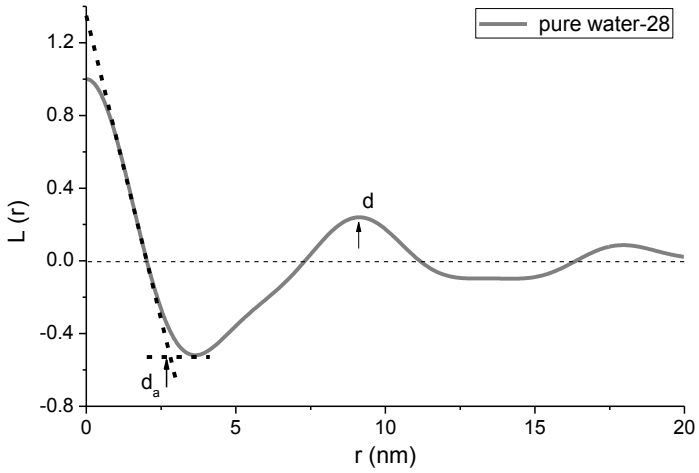

Fig. S2 Linear correlation function of the starch in pure water at 28 °C. d and d_a are the thicknesses of the semicrystalline lamellae and of the crystalline lamellae, respectively.